Acta Astronautica 99 (2014) 85–91

Contents lists available at ScienceDirect

Acta Astronautica

journal homepage: www.elsevier.com/locate/actaastro

Lunar surface heat flow mapping from radioactive elements measured by Lunar Prospector

Dan Zhang [a], Xiongyao Li [b,*], Qingxia Li [a], Liang Lang [a], Yongchun Zheng [c]

[a] Science and Technology on Multi-Spectral Information Processing Laboratory, Huazhong University of Science & Technology, Wuhan 430074, China

[b] The State Key Laboratory of Environmental Geochemistry, Institute of Geochemistry, Chinese Academy of Sciences, Guiyang 550002, China

[c] The National Astronomical Observatories, Chinese Academy of Sciences, Beijing 100012, China

ARTICLE INFO

Article history:
Received 1 June 2013
Received in revised form
5 October 2013
Accepted 25 January 2014
Available online 11 February 2014

Keywords:
Lunar surface heat flow
Radioactive elements
Heat production rate

ABSTRACT

An accurate estimate of global surface heat flow is important because it provides strong constraints on interior thermal model and understanding of the thermal state and geologic evolution of the Moon. In this paper, a distribution map of lunar surface heat flow is derived from calibrated Lunar Prospector gamma-ray spectrometer data (K, U and Th abundances). It shows that surface heat flow varies regionally from about 10.6 mW/m^2 to 66.1 mW/m^2, which is in the same order of magnitude as previous results. In the calculation, lunar surface heat flow includes the heat flow from the non-uniform distribution of radioactive elements K, U and Th and that from secular cooling of the Moon. The calculation of heat flow from radioactive elements is based on the assumption that the radioactive decay of K, U and Th on the Moon is the same as that on the Earth. The heat flow from secular cooling of the Moon is assumed to be equal to the global average radioactive heat flow. Firstly we construct a relationship between radioactive elements K, U and Th and lunar surface heat flow. The key parameter of the characteristic length scale in the relationship is determined by measured surface heat flow and Th abundances at Apollo 15 and 17 landing sites. Then the distribution of lunar surface heat flow is derived by combining other parameters such as lunar crustal thickness measured by Clementine and lunar crustal density. In addition, correlation analysis of the three radioactive elements is carried out due to the higher resolution of Th abundance and for ease of calculation.

1. Introduction

The Moon is a small planetary, and there is good reason to believe that it has lost most of its initial heat during its 4.6-b.y. history [1]. The present surface heat flow retains the information of lunar origin and evolution, which is considered a high priority for the lunar geophysical missions. Surface heat flow is defined as the amount of thermal energy coming out of a planet per unit surface area per unit time [2].

It is generally believed that the Moon is in steady state, because the Moon is lack of atmosphere, and has no obvious lithosphere movements [3]. Surface heat flow is presumptively equal to the heat production of the total abundances of radioactive elements below any given region on the Moon [4,5]. Binder [6] deduced surface heat flow ranging from about 3 mW/m^2 to more than 45 mW/m^2

* Corresponding author.
E-mail addresses: julia522x@163.com (D. Zhang), lixiongyao@vip.skleg.cn (X. Li), qingxia_li@hust.edu.cn (Q. Li), l_lang@mail.hust.edu.cn (L. Lang), zyc@nao.cas.cn (Y. Zheng).

http://dx.doi.org/10.1016/j.actaastro.2014.01.020
0094-5765

by analyzing the distribution characteristics of K, U and Th in different geological structures using the samples returned by the various Apollo and lunar missions, assuming that the abundances of the heat producing elements per unit mass in both the Earth and the Moon is the same. This assumption is not reasonable, because the Moon is enriched in refractory elements (Al, U, and Th) and FeO compared to the Earth [7], and this method provided the heat flow of five geological structures such as the KREEP zone. Yoshida et al. [8] assumed that the total Th abundance below a region is equal to a surface abundance multiplied by lunar crustal thickness, which is a constant. Then the surface heat flow of LUNAR-A two landing sites are estimated to be 30 mW/m^2 and 8 mW/m^2 by adopting the crustal thickness of 30 km deduced from the measured heat flow of the Apollo landing sites. This assumption that lunar crustal thickness is a constant at any region may not be valid because of the different processes of crust formation [9].

In addition to the heat flow by radioactive heat production, secular cooling of the Moon contributes to the surface heat flow [10]. In the lunar models, a radioactive heat production is typically only 70–80% of the surface heat flow [10]. The ratio between the heat production due to radioactive heating and the surface heat flow is defined as Urey ratio [11,12]. Based on a large number of thermal history calculations with parameter variations over a wide extent for the Moon and other planets, a Urey ratio of 0.5 is thought as a good and representative estimate that works surprisingly well for the terrestrial planets and many major satellites [12].

Based on radio observation on the Earth, lunar surface heat flow was measured to be 54 mW/m^2 [13]. So far there are only two surface heat flow measurements carried out on the Moon, i.e., the Apollo 15 and 17 landing sites, with revised values of 21 mW/m^2 and 14 mW/m^2, based on monitoring intervals of 3.5 and 2 years respectively [4]. Currently the two existing measurements of lunar surface heat flow are unlikely to be representative of the global surface heat flow because they are located at geographical/geological boundaries [14,15].

Thus, mapping of lunar surface heat flow is important. In this paper, we derive the distribution of lunar surface heat flow by considering the heat flow produced by radioactive decay of K, U and Th in the crust, as well as the heat flow from the cooling of the Moon. The heat flow from secular cooling of the Moon is assumed to equal to the global average radioactive heat flow, based on the Urey ratio of 0.5. Because K, U and Th are unevenly distributed in the KREEP [potassium (K), rare earth elements (REE), phosphorus (P)] in the crust layer [6,16], lunar surface heat flow varies regionally.

In this paper, we firstly introduce the abundances of K, U and Th using Prettyman et al. [17] calibrated data and the abundance of Th using Lawrence et al. [18] calibrated data from Lunar Prospector measurements; then we present a method for calculating the heat flow produced by radioactive elements K, U and Th, including the correlation analysis among K, U and Th and the determination of the characteristic length scale. Finally, the global distribution of lunar surface heat flow is derived.

2. Radioactive elements distribution

Launched onboard the Lunar Prospector in 1998, the gamma-ray spectrometer is a more advanced system than that was flown on the Apollo missions and provides global maps of the elemental composition of the surface layer of the Moon. It determines the abundance of main elements with a few tens of centimeters (~20 cm) of the lunar surface [19]. The main elements mapped are U, Th, K, Fe, Ti, O, Si, Al, Mg and Ca. Knowledge of the abundances of these elements over the entire lunar surface will aid in understanding of lunar formation and evolution [20]. K, U and Th are trace elements which are most abundant in the KREEP [21]. Mapping the locations and concentrations of KREEP deposits is important to lunar science as it is believed that the material developed late in the formation of the lunar crust and upper mantle, and thus can help define how the crust and mantle formed and evolved. In addition, K, U and Th are radioactive elements, and constrain the lunar surface heat flow.

The gamma-ray spectrometer acquired gamma ray and neutron spectra at two altitudes (30- and 100 km) over the whole moon [17]. High-altitude spectra data were measured from January 16, 1998, to December 19, 1998. Low-altitude spectra data were measured from December 19, 1998 to July 31, 1999 [15]. The footprint of gamma-ray spectrometer is around 5° by 5° at the equator.

The raw spectral data were corrected for variations in gain, dead time, and the flux of galactic cosmic rays as a function of time. Converting gamma-ray spectrometer counts into absolute abundances for all the measurable elements requires a series of involved detector modeling and spectral fitting procedures. The abundance of radioactive elements K, U and Th was determined by fitting the gamma ray spectrum in the 700–9000 keV region using library least squares. The spectra was acquired at high altitude and binned on 5° by 5° [17].

Here the maps of abundances of K, U and Th, as shown in Figs. 1, 2 and 3 respectively, are derived from gamma ray spectra measured by the gamma-ray spectrometer [17]. From the maps, it is shown that K, U and Th are concentrated primarily on the nearside within and around the western maria. The distributions of K, U and Th look similar. Lawrence et al. [18] optimized the measured spatial resolution to the limit of the orbital gamma-ray technique by smoothing the data using an empirically determined gamma-ray response function and provided

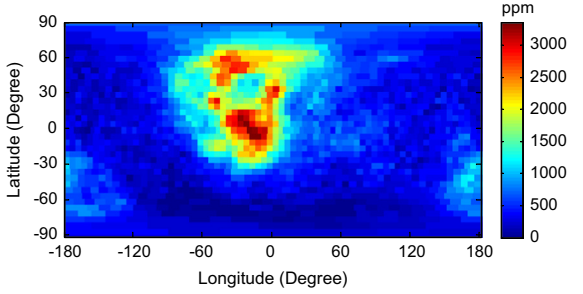

Fig. 1. K abundance (ppm) using the Prettyman et al. [17] calibrated data from Lunar Prospector measurements (1° resolution).

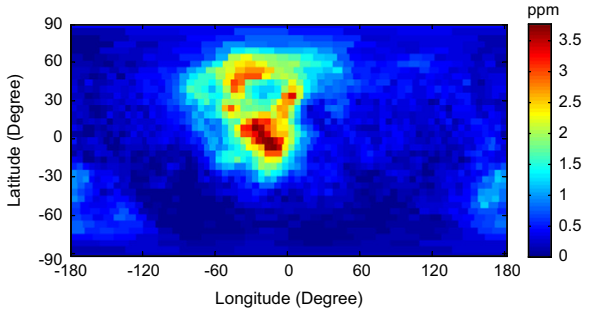

Fig. 2. U abundance (ppm) using the Prettyman et al. [17] calibrated data from Lunar Prospector measurements (1° resolution).

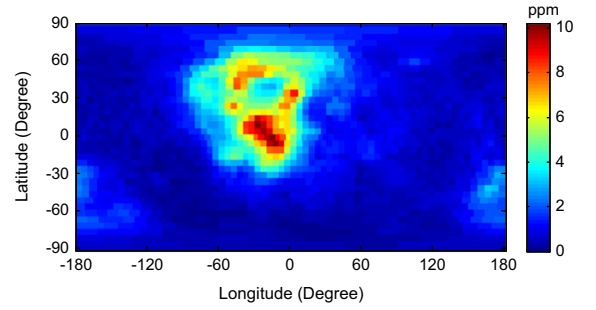

Fig. 3. Th abundance (ppm) using the Prettyman et al. [17] calibrated data from Lunar Prospector measurements (1° resolution).

the high-altitude and low-altitude Th abundance using pixels of 0.5° by 0.5° that were substantially smaller than the expected footprint of gamma-ray spectrometer. The distribution of low-altitude Th abundance is shown in Fig. 4. The Lunar Prospector counting rate measurements are in agreement with sample measurements. The uncertainties for both the high-altitude and low-altitude Th abundance are less than 0.5 ppm [22]. The low-altitude Th abundance has distinctly better surface resolution than the high-altitude Th abundance [22]. We binned the Th abundance of 0.5° by 0.5° onto 1° by 1° for calculating the surface heat flow in the next section.

3. Calculation method

The heat flow produced by K, U and Th is closely related to heat production rate. The relationship between surface heat flow and heat production rate in the continental crust has been investigated systematically [23–25], as well as the relationship between heat production rate and abundances of K, U and Th [26]. Assuming that the radioactive decay is identical both in the Earth and the Moon, a relationship between lunar surface heat flow and radioactive elements K, U and Th is derived.

In order to obtain lunar surface heat flow from measured K, U and Th, a method is presented in the paper. Firstly, we construct a relationship between radioactive elements (K, U and Th) and lunar surface heat flow. Due to the higher resolution of Th abundance and for ease of calculation, the relationship is simplified to the form that lunar surface heat flow is only related to Th, on the basis of the correlations among K, U and Th. The characteristic

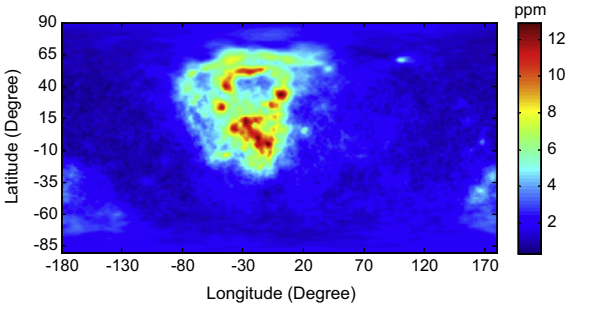

Fig. 4. Th abundance (ppm) using the Lawrence et al. [18] calibrated data from Lunar Prospector measurements (0.5° resolution).

length scale, which is an important parameter in the relationship, is determined by lunar crustal thickness, the measured heat flow and abundance of Th at Apollo 15 and 17 landing sites. Finally, the heat flow produced by radioactive elements is calculated, with the parameters of the crustal density, characteristic length scale, abundance of Th and lunar crustal thickness substituted in the relationship. In addition to the heat flow by radioactive heat production, secular cooling of the moon contributes to lunar surface heat flow. The ratio of heat flow by radioactive heat production to surface heat flow is assumed to be 0.5, which is a good and representative estimate for the Moon [12]. Because the mechanisms of radioactive heat and heat produced from secular cooling of the Moon are different, here we assume the heat flow from secular cooling of the Moon is equal to the global average heat flow produced by radioactive elements. Summing the two parts of heat flow, the global distribution of lunar surface heat flow is derived. Calculation process in detail is introduced as follows.

The heat production rate of a rock sample is calculated by summing the contributions of each element, which is expressed as [26]

$$P_t = 10^{-11}\rho(9.52C_U + 2.56C_{Th} + 3.48C_K) \quad (1)$$

where P_t is the heat production rate of radioactive elements K, U and Th with the unit of $\mu W/m^3$; ρ is the density of lunar rocks, with the unit of g/cm^3; C_U and C_{Th} are the abundances of U and Th in ppm, respectively; and C_K is the abundance of K in percent.

Returned soil and rock samples from the Moon show that Th and K abundances are correlated [27]. Such a correlation is also found in the distributions of K, U and Th measured by Lunar Prospector (Figs. 1, 2 and 3). The correlation between Th and K is shown in Fig. 5. The fitted line has a slope of 0.0344 with a correlation coefficient of 0.957. The correlation between Th and U is shown in Fig. 6. The fitted line has a slope of 351.3 with a correlation coefficient of 0.9521.

It is shown from Figs. 5 and 6 that K and Th have a strong correlation, as well as U and Th. The resolution of calibrated Th abundance is 0.5° by 0.5°, which is much higher than the resolution of 5° by 5° for U and K abundances. Thus the abundance of Th is substituted for that of K and U in Eq. (1). The data are binned onto 1° by 1° for calculation.

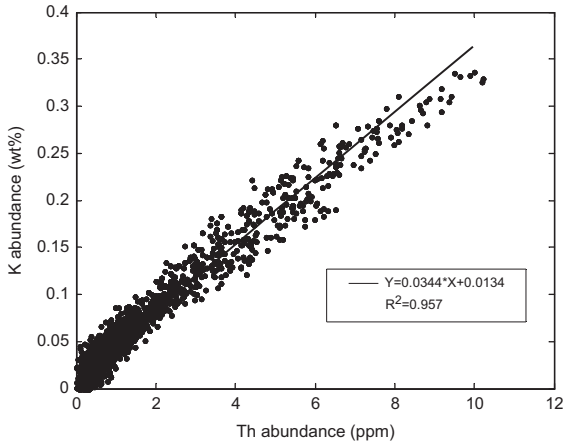

Fig. 5. Abundance of K versus that of Th measured by Lunar Prospector.

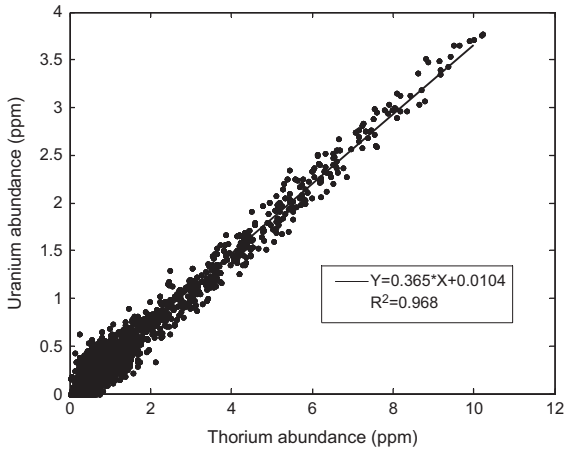

Fig. 6. Abundance of U versus that of Th measured by Lunar Prospector.

Based on the correlations of K, U and Th, Eq. (1) can be simplified as

$$P_t = 10^{-11}\rho(6.15C_{\mathrm{Th}} + 0.15) \tag{2}$$

The vertical distribution of the radioactive elements in the crust is assumed to decrease exponentially with depth, referring to the vertical distribution of those on the Earth [27], while the surface distribution of those elements are obtained by Lunar Prospector. Thus the heat production rate on the Moon at any depth is given by

$$P_t(z) = P_t e^{-z/h_r} \tag{3}$$

where z is the depth; $P_t(z)$ and P_t denote heat production rate at the depth z and on the surface, respectively; and h_r, the characteristic length scale, is defined as the depth at which heat production rate decreases to $1/e$ of the surface heat production rate [28].

The heat production rate denotes the heat produced by radioactive elements in a unit volume. Integrated along the depth, the heat flow produced by radioactive elements is expressed as

$$q_{crust} = \int_0^H P_t(z)dz = \int_0^H P_t e^{-z/h_r} dz \tag{4}$$

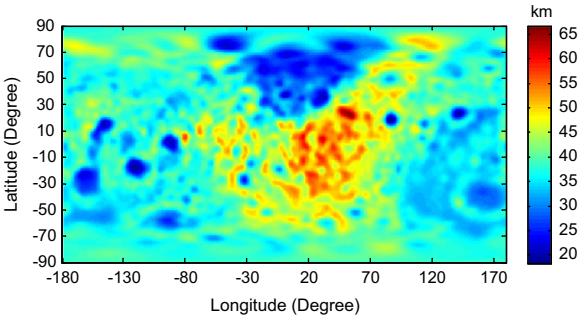

Fig. 7. Distribution of lunar crustal thickness (km) measured by Clementine.

where q_{crust} denotes the heat flow produced by radioactive elements; H is the thickness of lunar crust. Then P_t is substituted in Eq. (4). The heat flow produced by radioactive elements is determined by

$$q_{crust} = 10^{-11}\rho h_r(6.15C_{\mathrm{Th}} + 0.15)\left(1 - e^{-H/h_r}\right) \tag{5}$$

Eq. (5) describes the energy directly produced by radioactive heat resources. After considering the contribution from secular cooling of the Moon, lunar surface flow is given by

$$Q_s = 10^{-11}\rho h_r(6.15C_{\mathrm{Th}} + 0.15)\left(1 - e^{-H/h_r}\right) + Q_{mantle} \tag{6}$$

where Q_s is the surface heat flow on the Moon; Q_{mantle} is the heat flow due to secular cooling of the Moon. Under the assumption that the ratio of radioactive heat flow to lunar surface heat flow is 0.5 [12], it is reasonable to think that Q_{mantle} is equal to the global average heat flow produced by radioactive elements.

Eq. (5) provides the estimation for heat flow produced by radioactive elements K, U and Th. Eq. (6) provides the estimation for lunar surface heat flow. Calculations can be carried out by substituting the parameters into Eq. (6). ρ is the average lunar crustal density with a value of 2.8 g/cm^3 [28–30]. H is the thickness of lunar crust.

The global lunar crustal thicknesses distribution can be calculated from the topography and gravity data by Clementine (http://pds-geosciences.wustl.edu/geodata/clem1-gravity-topo-v1/cl_xxxx/gravity/thickgrd.dat), as shown in Fig. 7.

h_r, The characteristic length scale, can be determined by lunar crustal thickness, the measured heat flow and Th abundances at Apollo 15 and 17 landing sites, according to Eq. (5). It is expressed as

$$\frac{1 - e^{-H_1/h_r}}{1 - e^{-H_2/h_r}} = \frac{q_{crust\_15}(6.15C_{\mathrm{Th}\_17} + 0.15)}{q_{crust\_17}(6.15C_{\mathrm{Th}\_15} + 0.15)} \tag{7}$$

where H_1 and H_2 are lunar crustal thicknesses at Apollo 15 and 17 landing sites, respectively; q_{crust_15}, q_{crust_17} are the heat flow produced by radioactive elements, which are equal to a half of the measured surface heat flow with values of 21 mW/m^2 and 14 mW/m^2 at Apollo 15 and 17 landing sites [4]; C_{Th_15}, C_{Th_17} are the abundances of radioactive element Th at Apollo 15 and 17 landing sites, respectively.

Table 1
Parameters for Eq. (7) at Apollo 15 and 17 landing sites.

	Measured surface heat flow (mW/m^2) [4]	Radioactive heat flow (mW/m^2)	Th abundance (ppm) [17]	Lunar crustal thickness (km)
Apollo15	21	10.5 (q_{crust_15})	5.05 (C_{Th_15})	31.85 (H_1)
Apollo17	14	7 (q_{crust_17})	2.64 (C_{Th_17})	49.25 (H_2)

Note: The lunar crustal thickness values in column 4 are measured by Clementine.

At Apollo 15 and 17 landing sites, surface heat flow was obtained by multiplying the temperature gradient by the thermal conductivity. Because lunar surface temperatures are strongly affected by the 18.6-year precession of the lunar orbit, they will surely affect the subsurface temperature profile. The Apollo data were obtained at relatively shallow depths (1.6–2.3 m) for duration (~6 years) much shorter than the precession-controlled period of the surface temperature fluctuation [2,31]. As the transient noise was neglected in the initial heat flow analyses, the reliability of the measured temperatures needs to be further confirmed [32–34]. In addition, Langseth et al. [4] derived average thermal conductivities of the regolith columns penetrated by the sensors by modeling the process of diurnal and annual temperature signals propagating downward instead of in-situ thermal conductivity data in their determination of the heat flow values. Different approaches to determine the conductivity yielded discordant results. The cause of the discrepancy between the model-derived and the in-situ thermal conductivities needs to be investigated in the future [31–35].

Currently there are only two measured values of lunar surface heat flow at Apollo 15 and 17 landing sites, which were revised by removing the diurnal, annual, and short-term transient signatures from measured temperature series [4]. Though the accuracy of measured surface heat flow can be improved, the values are still reasonable and valuable. The low measured heat flow value is consistent with the Moon's small size, which favors rapid, early cooling of the interior [36]. Using the measured lunar surface heat flow, h_r can be determined.

The parameters needed in Eq. (7) are listed in Table 1. With these parameters, h_r is estimated to be 35.70 with the unit of km.

With the values for the characteristic length scale h_r, lunar crustal density ρ, the abundance of Th C_{Th}, and lunar crustal thickness H, the heat flow produced by radioactive elements can be calculated from Eq. (5). Then the heat flow from secular cooling of the moon can be obtained by averaging. Summing the two parts of heat flow, the global distribution of lunar surface heat flow can be obtained by Eq. (6).

4. Results

Based on Eq. (5) with lunar crustal density ρ, the characteristic length scale h_r, the Th abundance C_{Th}, measured by Lunar Prospector and lunar crustal thickness H, the heat flow distribution produced by the radioactive elements K, U and Th is calculated, as shown in Fig. 8. The heat flow produced by the radioactive elements ranges from 1.5 mW/m^2 to 56.9 mW/m^2. The global average heat flow is 9.1 mW/m^2; that is to say, the heat flow from secular cooling of the Moon is 9.1 mW/m^2, in view of the Uray ratio of 0.5. Based on Eq. (6), lunar surface heat flow is derived, as shown in Fig. 9.

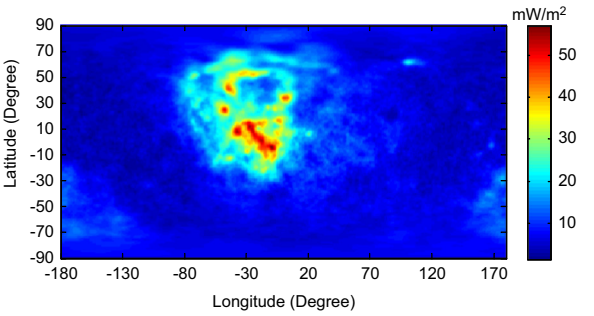

Fig. 8. Distribution of the heat flow produced by radioactive elements K, U and Th measured by Lunar Prospector.

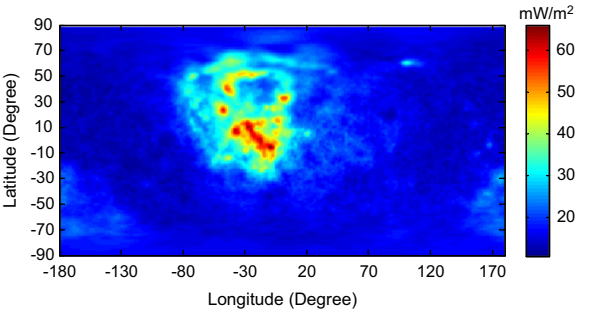

Fig. 9. Distribution of lunar surface heat flow, using Urey ratio.

From Fig. 9, it can be seen lunar surface heat flow are as low as 10.6 mW/m^2 in the polar regions while they are up to 66.1 mW/m^2 near the equator. The average heat flow is 18.3 mW/m^2. The distribution of surface heat flow shows lunar distribution signatures with close similarity to those seen in the distributions of K, U and Th. The heat flow is concentrated primarily on the nearside within and around the western maria, with an average value of 33.3 mW/m^2. The highest surface heat flow extends from the southern edge of Mare Imbrium near Copernicus to near the Apollo 14 landing site at Fra Mauro. In addition, the regions including the eastern edge of Oceanus Procellarum, the western edge of Sinus Iridum, and northern part near the Luna 2, have an average surface heat flow of 46.6 mW/m^2. The distribution of lunar heat surface is closely related to that of KREEP.

In addition, all the lunar landings and photographic investigations show that the entire lunar surface consists of a regolith layer that completely covers the underlying bedrock [1]. In the calculation, we choose the parameter of crustal density with a value of 2.8 g/cm^3 to calculate lunar surface heat flow, which has a deviation because the density of lunar regolith is 1.8 g/cm^3. The heat flow produced from lunar regolith layer is estimated to be 0.4×10^{-3}–14.2×10^{-3} mW/m^2, assuming $\rho=1.8$ g/cm^3,

and the average thickness of lunar regolith ranges from 5 m to 10 m. Thus, the heat flow from the whole regolith layer is less than 1.63×10^{-2} mW/m^2. It is neglected because the surface heat flow from lunar interior is about 10.6 mW/m^2 to 66.1 mW/m^2.

Without considering the heat flow from secular cooling of the Moon, the heat flow produced by radioactive elements are in the same order of magnitude as those calculated in [6] referring to the heat flow of the Earth and returned sample analysis from the Moon, which are about 3 mW/m^2 to more than 45 mW/m^2. Summing the heat flow from secular cooling of the Moon, the average lunar heat flow on the nearside is 12 mW/m^2, which is lower than the value of 54 mW/m^2 based on radio observation on the Earth [13].

5. Conclusion

Lunar surface heat flow provides important constraints on the interior thermal model and understanding of the thermal state and geologic evolution of the Moon. Using the abundances of radioactive elements K, U and Th measured by Lunar Prospector, we construct a relationship between the abundances of radioactive elements and lunar surface heat flow, the part of which from secular cooling of the moon is assumed to be equal to the global average heat flow produced by radioactive elements, based on Urey ratio of 0.5. The key parameter of the characteristic length scale is determined by measured surface heat flow at Apollo 15 and 17 landing sites. Then the lunar crustal density, lunar crustal thickness, and Th abundance are combined to calculate the distribution of lunar surface heat flow.

The distribution indicates the lunar surface heat flow varies regionally from about 10.6 mW/m^2 to 66.1 mW/m^2. The average heat flow is 18.3 mW/m^2. The heat flow is concentrated primarily on the nearside within and around the western maria, with an average value of 33.3 mW/m^2. The distribution of lunar heat surface is closely related to that of KREEP.

In addition, the radioactive elements K, U and Th measured by Lunar Prospector were correlative. These data were correlatively analyzed. The resolution of calibrated Th abundance is 0.5° by 0.5°, which is much higher than the resolution of 5° by 5° for U and K abundances. Thus, the abundance of Th is substituted for that of K and U for improving the accuracy and simplifying calculation.

Due to the fact that the current understanding of the internal structure of the Moon is mainly based on Apollo seismic data, in which the useful seismic waves penetrate to a depth of about 400 km. The lunar model for calculating the heat flow from secular cooling of the Moon is complicated and lacks sufficient accurate model parameters. Further improvements are necessary for more accurate estimation of lunar surface heat flow.

Acknowledgment

We gratefully thank the reviewers for their careful reading and valuable suggestions. This work is supported in part by the National High Technology Research and Development Program of China (863 Program) with a Contract no. 2010AA122204 and in part by the National Natural Science Foundation of China with Contract nos. 40904051, 41001195, 41275032.

References

[1] G.H. Heiken, D.T. Vaniman, B.M. French, Lunar Sourcebook: A User's Guide to the Moon, Cambridge University Press, London, 1991.
[2] W.S. Kiefer, Lunar heat flow experiments: science objectives and a strategy for minimizing the effects of lander-induced perturbations, Planet. Sp. Sci. 60 (1) (2012) 155–165.
[3] A. Hagermann, Planetary heat flow measurements, Philos. Trans. R. Soc. A: Math., Phys. Eng. Sci. 363 (1837) (2005) 2777–2791.
[4] M.G. Langseth Jr., S.J. Keihm, K. Peters, Revised lunar heat-flow values, in: Proceedings of the Lunar and Planetary Science Conference, vol. 7, 1976, pp. 3143–3171.
[5] D.L. Turcotte, F.A. Cooke, R.J. Willeman, Parameterized convection within the moon and the terrestrial planets, in: Proceedings of the 10th Lunar and Planetary Science Conference, vol. 28, 1979, pp. 2375–2392.
[6] A.B. Binder, On the heat flow of a gravitationally-differentiated moon of fission origin, Moon 14 (2) (1975) 237–245.
[7] D.J. Lawrence, W.C. Feldman, B.L. Barraclough, A.B. Binder, R. C. Elphic, S. Maurice, T.H. Prettyman, Thorium abundances on the lunar surface, J. Geophys. Res.: Planets (1991–2012) 105 (E8) (2000) 20307–20331.
[8] S. Yoshida, S. Tanaka, A. Hagermann, M. Hayakawa, A. Fujimura, H. Mizutani, Derivation of globally averaged lunar heat flow from the local heat flow values and the thorium distribution at the surface: expected improvement by the LUNAR – a mission, in: Proceedings of the 32nd Lunar and Planetary Science Conference, 12–16 March, Houston, Texas, USA, 2001.
[9] Y. Ishihara, S. Goossens, K. Matsumoto, H. Noda, H. Araki, N. Namiki, H. Hanada, T. Lwata, S. Tazawa, S. Sasaki, Crustal thickness of the moon: implications for farside basin structures, Geophys. Res. Lett. 36 (19) (2009). L19202, 4 pp.
[10] G. Schubert, D. Stevenson, P. Cassen, Whole planet cooling and the radiogenic heat source contents of the Earth and Moon, J. Geophys. Res.: Solid Earth 85 (B5) (1980) 2531–2538.
[11] T. Nakagawa, P.J. Tackley, Influence of magmatism on mantle cooling, surface heat flow and Urey ratio, Earth Planet. Sci. Lett. 329 (2012) 1–10.
[12] T. Spohn, D. Breuer, Surface heat flow, radiogenic heating, and the evolution of the Moon, in: Proceedings of the EGS General Assembly Conference Abstracts, vol. 27, 2002, pp. 6000.
[13] V.D. Krotikov, V.S. Troitskii, Detecting heat flow from the interior of the Moon, Sov. Astron. 7 (1964) 822–826.
[14] S.P. Huang, W.S. Kiefer, C.R. Neal, N. Kömle, M. Banaszkiewicz, M.A. Wieczorek, S. Tanaka, Three deployment options for the heat flow component of the long-lived lunar geophysics instrument package, in: Proceedings of the Lunar and Planetary Institute Science Conference Abstracts, vol. 39, 2008, pp. 1162.
[15] M.A. Wieczorek, R.J. Phillips, The "Procellarum KREEP Terrane": implications for mare volcanism and lunar evolution, J. Geophys. Res.: Planets (1991–2012) 105 (E8) (2000) 20417–20430.
[16] B.L. Jolliff, J.J. Gillis, L.A. Haskin, R.L. Korotev, M.A. Wieczorek, Major lunar crustal terranes: surface expressions and crust–mantle origins, J. Geophys. Res.: Planets 105 (E2) (2000) 4197–4216.
[17] T.H. Prettyman, W.C. Feldman, D.J. Lawrence, G.W. McKinney, A.B. Binder, R.C. Elphic, O.M. Gasnault, S. Maurice, K.R. Moore, Library least squares analysis of Lunar Prospector gamma-ray spectra, in: Proceedings of the Lunar and Planetary Science Abstract, 2002.
[18] D.J. Lawrence, R.C. Elphic, W.C. Feldman, O. Gasnault, I. Genetay S. Maurice, T.H. Prettyman, Small-area thorium enhancements on the lunar surface, in: Proceedings of the Lunar and Planetary Institute Science Conference Abstracts, vol. 33, 2002, pp. 1970.
[19] T.H. Prettyman, J.J. Hagerty, R.C. Elphic, W.C. Feldman, D.J. Lawrence, G.W. McKinney, D.T. Vaniman, Elemental composition of the lunar surface: analysis of gamma ray spectroscopy data from lunar prospector, J. Geophys. Res.: Planets 111 (E12) (2006). E12007, 41 pp.
[20] M.A. Wieczorek, R.J. Phillips, Potential anomalies on a sphere: applications to the thickness of the lunar crust, J. Geophys. Res. 103 (1998) 1715–1724. (EI).
[21] A.B. Binder, Lunar Prospector: overview, Science 281 (5382) (1998) 1475–1476.

[22] D.J. Lawrence, W.C. Feldman, B.L. Barraclough, A.B. Binder, R. C. Elphic, S. Maurice, D.R. Thomsen, Global elemental maps of the moon: the lunar prospector gamma-ray spectrometer, Science 281 (1998) 1484–1489.
[23] P.C. England, E.R. Oxburg, S.W. Richardson, Heat refraction in and around granites in north-east England, Geophys. J. R. Astron. Soc. 62 (2) (1980) 439–455.
[24] C. Jaupart, Horizontal heat transfer due to radioactivity contrasts: causes and consequences of the linear heat flow heat production relationship, Geophys. J. Int. 75 (2) (1983) 411–431.
[25] G. Vasseur, R.N. Singh, Effects of random horizontal variations in radiogenic heat source distribution on its relationship with heat flow, J. Geophys. Res.: Solid Earth 91 (B10) (1986) 10397–10404.
[26] L. Rybach, Determination of heat production rate, Handbook of Terrestrial Heat-Flow Density Determination, vol. 486, 1988, R. Haenel, L. Rybach, L. Stegena (Eds.), Kluwer Academic Publishers, Dordrecht, pp. 125–142.
[27] R.L. Korotev, Concentrations of radioactive elements in lunar materials, J. Geophys. Res. 103 (1998) 1691–1701(EI) 103 (1998) 1691–1701.
[28] M. Sandiford, M. Sandra, Tectonic feedback and the ordering of heat producing elements within the continental lithosphere, Earth and Planet. Sci. Lett. 204 (1) (2002) 133–150.
[29] M.T. Zuber, D.E. Smith, F.G. Lemoine, G.A. Neumann, The shape and internal structure of the moon from the Clementine mission, Science 266 (5192) (1994) 1839–1843.
[30] R.R. Von Frese, M.B. Jones, J.W. Kim, J.H. Kim, Analysis of anomaly correlations, Geophysics 62 (1) (1997) 342–351.
[31] S. Nagihara, P.T. Taylor, M.B. Milam, P.D. Lowman, Y. Nakamura, Designing heat flow experiments for future lunar missions, in: Proceedings of the Lunar and Planetary Institute Science Conference Abstracts, vol. 39, 2008, pp. 1087.
[32] M.A. Wieczorek, S. Huang, A reanalysis of Apollo 15 and 17 surface and subsurface temperature series, in: Proceedings of the 37th Annual Lunar and Planetary Science Conference, vol. 37, 2006, pp. 1682.
[33] S. Nagihara, P.T. Taylor, D.R. Williams, Y. Saito, Long-term warming of surface and subsurface temperatures observed at Apollo 15 and 17 sites: implications for future lunar geophysical missions, Lun. Planet. Inst. Contrib. 1530 (2010) 3008.
[34] Y. Saito, S. Tanaka, J. Takita, K. Horai, A. Hagermann, Lost Apollo heat flow data suggest a different lunar bulk composition, in: Proceedings of the Lunar and Planetary Science Conference, vol. 16, 2006, pp.158–164.
[35] M. Grott, J. Knollenberg, C. Krause, Apollo lunar heat flow experiment revisited: a critical reassessment of the in situ thermal conductivity determination, Eur. Planet. Sci. Congr. Abstr. 5 (2010).
[36] C.R. Neal, L. Hood, S. Huang, S. Sakimoto, W. Kiefer, J. Weinberg, The case for a long-lived global lunar geophysical network-2: magnetic and heat flow data, in: Proceedings of the Lunar and Planetary Institute Science Conference Abstracts, vol. 38, 2007, pp. 2428.